Ultraviolet continuum spectroscopy of vibrationally excited ozone

S. M. AdlerGolden, E. L. Schweitzer, and J. I. Steinfeld

Citation: J. Chem. Phys. **76**, 2201 (1982); doi: 10.1063/1.443293
View online: http://dx.doi.org/10.1063/1.443293
View Table of Contents: http://jcp.aip.org/resource/1/JCPSA6/v76/i5
Published by the American Institute of Physics.

Ultraviolet continuum spectroscopy of vibrationally excited ozone

S. M. Adler-Golden,[a] E. L. Schweitzer, and J. I. Steinfeld

Department of Chemistry, Massachusetts Institute of Technology, Cambridge, Massachusetts 02139
(Received 5 November 1981; accepted 16 November 1981)

A model is presented for the Hartley ultraviolet spectrum of vibrationally excited ozone based upon infrared–ultraviolet double resonance spectroscopy and previous temperature-dependent absorption measurements. The double-resonance transient arises from a 3500 cm^{-1} red shift of the absorption spectrum of ozone excited into the stretching vibrational states, with respect to the ground vibrational state. The double-resonance method is used to study relaxation kinetics of vibrationally excited ozone and to measure infrared energy deposition resulting from CO_2 laser pumping. The energy deposition is found to scale linearly with sample pressure and with infrared fluence, except for excitation on-resonance, which is strongly saturated. The UV spectral model is also used to calculate the wavelength and temperature dependence of the $O(^1D)$ photodissociation quantum yield, which is an important component of stratospheric photochemistry.

I. INTRODUCTION

The ultraviolet absorption spectrum of ozone is among the most important features of that molecule, one of the key species in stratospheric photochemistry.[1] Despite extensive study, many questions remain concerning the Hartley continuum, a strong and nearly structureless absorption feature in the vicinity of 200–300 nm. Another poorly understood yet important subject concerns properties of vibrationally excited ozone, an abundant species formed in the $O+O_2$ $[+M]$ recombination process.[2–4] The ultraviolet spectrum of vibrationally excited ozone is a potentially critical ingredient in stratospheric modeling.

In this article, we discuss recent experimental and theoretical work which sheds further light on the ultraviolet spectroscopy and kinetic properties of vibrationally excited ozone. The experimental technique utilized is infrared–ultraviolet double resonance spectroscopy, in which the asymmetric stretching mode (ν_3) is pumped by a pulsed CO_2 laser and the Hartley absorption band is probed by a continuous UV source. The apparatus has been described previously[5]; minor modifications are mentioned herein. Similar experiments have also been performed independently by McDade and McGrath.[6,7] The IRUVDR work, combined with absorption spectrum data and *ab initio* calculations, yields a self-consistent model for the Hartley band spectroscopy of vibrationally excited ozone. Application of this model enables us to determine rate constants for vibrational energy transfer, obtain information on the IR laser excitation process, and evaluate the hypothetical influence of vibrational excitation on stratospheric ozone photolysis in the ultraviolet region.

II. SPECTROSCOPIC MODEL

Portions of the potential energy surfaces for the electronic states involved in the Hartley ultraviolet transition have been obtained from *ab initio* computations[8]; thus, Franck–Condon intensity calculations on the Hartley band are possible in principle. Unfortunately, such spectral calculations have yet to be performed, one major difficulty being the strong coupling between the two stretching motions on the upper surface. Nevertheless, a qualitative understanding of the shape of the Hartley band and its dependence upon vibrational excitation may be readily obtained from simple arguments. Let us assume that the total vibrational wave function may be approximated as

$$\psi(q_1, q_2, q_3) = \psi_{\text{bend}}(q_2)\,\psi_{\text{stretch}}(q_1, q_3)\,, \tag{1}$$

and that the lower and upper potential functions satisfy

$$V_u(q_1, q_2, q_3) - V_l(q_1, q_2, q_3) = \Delta V_{\text{bend}}(q_2) + \Delta V_{\text{stretch}}(q_1, q_3)\,, \tag{2}$$

where q_2 is the bending coordinate and q_1, q_3 are the symmetric and asymmetric stretching coordinates, respectively. The essence of these equations is that bending vibrational motion is assumed to be decoupled from the stretching motions. The mean transition energy of the spectrum $\langle h\nu\rangle$ is then given [see Eq. (4) of Ref. 9] by

$$\langle h\nu\rangle = \langle\psi_{\text{bend}}|\,\Delta V_{\text{bend}}\,|\psi_{\text{bend}}\rangle + \langle\psi_{\text{stretch}}|\,\Delta V_{\text{stretch}}\,|\psi_{\text{stretch}}\rangle\,. \tag{3}$$

The shift in the spectrum upon vibrational excitation in the bending mode may thus be written as

$$\langle h\nu\rangle_{010} - \langle h\nu\rangle_{000} = \langle\psi^1_{\text{bend}}|\,\Delta V_{\text{bend}}\,|\psi^1_{\text{bend}}\rangle - \langle\psi^0_{\text{bend}}|\,\Delta V_{\text{bend}}\,|\psi^0_{\text{bend}}\rangle\,, \tag{4}$$

where the superscript refers to the bending quantum number. This expression may be evaluated from Eq. (2a) of Ref. 9 using the vibrational frequencies derived from the *ab initio* calculations, yielding a result of -150 cm^{-1}. Thus, one may conclude that excitation into the bending mode will cause only a small red shift in the spectrum. The small magnitude of the shift results from both ground and excited electronic state bending frequencies being roughly similar. As it is also predicted from the *ab initio* calculations (and has been demonstrated experimentally[10]) that the equilibrium

[a] Present address: Spectral Sciences Inc., Burlington, Mass. 01803.

 0021-9606/82/052201-09$02.10

bond angles are also quite similar in the two states, only a slight change in spectral breadth with bending excitation is expected. Thus, both (010) and (000) states of ozone should have Hartley absorption spectra of very similar shapes.

On the other hand, excitation into either of the stretching modes is predicted to have a very large effect upon the Hartley band. The upper potential has a double minimum along the q_3 direction,[8] hence excitation into the (001) state should yield a substantial red shift.[9] Also, at large displacements from the electronic ground state geometry, the upper surface should have a dissociative trench along the directions corresponding to the stretching of each bond separately; these directions are admixtures of both q_1 and q_3 coordinates. Thus, one expects that at the long-wavelength end of the spectrum, which reflects Franck–Condon overlap in the trench region, both (100) and (001) states may have comparably large absorption coefficients.

A spectral model for the Hartley band is suggested by the above discussion and may be summarized as follows. Denoting P_{ijk} as the fractional population of ground electronic state ozone in the (ijk) vibrational state, having an absorption coefficient $\epsilon_{ijk}(\nu)$, then at low excitations

$$\epsilon = P_{000}\epsilon_{000} + P_{010}\epsilon_{010} + P_{100}\epsilon_{100} + P_{001}\epsilon_{001} , \quad (5)$$

where from the above arguments $\epsilon_{000} \approx \epsilon_{010}$. Furthermore, under conditions where P_{100} and P_{001} are in equilibrium, their populations are in roughly the same relative proportion, at and above room temperature. Therefore, we may write

$$P_{100}\epsilon_{100} + P_{001}\epsilon_{001} \approx (P_{100} + P_{001})\epsilon^* , \quad (6)$$

where ϵ^* is the population-weighted average extinction coefficient for the first excited stretching modes. The final result is

$$\epsilon = (P_{000} + P_{010})\epsilon_{000} + (P_{100} + P_{001})\epsilon^* , \quad (7)$$

which is a two-parameter approximation to the vibrationally excited Hartley continuum.

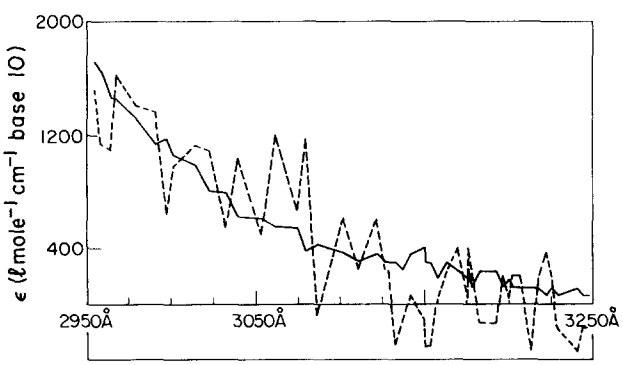

FIG. 1. The absorption spectrum of (100) plus (001) excited ozone ϵ^* in the 2950–3250 Å region. Dashed curve is the solution of three simultaneous equations based on Eq. (8), using spectra of 200, 300, and 333 K from Ref. 11. Solid curve is obtained by setting $\epsilon_{000} = \epsilon_{010}$ and using only the 200 and 333 K spectra.

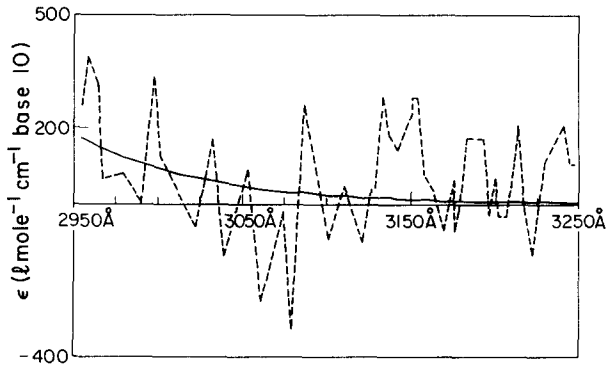

FIG. 2. Absorption spectra of ozone in the 2950–3250 Å region, obtained by solution of three simultaneous equations based on Eq. (8). Solid curve is ϵ_{000}, dashed curve is ϵ_{010}.

The spectral model expressed by Eq. (7) is subject to experimental verification. Several independent tests which lend support to this model are described below.

A. Temperature dependence

The most comprehensive study of the temperature-dependence of the Hartley band is the work of Simons *et al.*[11] who measured spectra at 200, 300, and 333 K. Bair has provided us with the absorption coefficient data in tabular form, which is used in the following calculations. From Eqs. (5) and (6) we can obtain a three-parameter equation

$$\epsilon = P_{000}\epsilon_{000} + P_{010}\epsilon_{010} + (P_{000} + P_{001})\epsilon^* , \quad (8)$$

from which it is possible to solve explicitly for ϵ_{000}, ϵ_{010}, and ϵ^* given the three experimental spectra. In practice, the solutions are very sensitive to experimental errors, such as normalization of the spectra, due to the weakness of the temperature dependence. For this reason, we have restricted the analysis to the spectral region where the temperature effect is greatest. The solutions of Eq. (8) are depicted in Figs. 1 and 2. The "noise" arises from the small amount of structure present in the original spectra. It is observed that, to within the noise level, the hypothesis that $\epsilon_{000} \approx \epsilon_{010}$ is confirmed. The conjecture by Bair and others[11,12] that ϵ_{010} is red shifted by ~ 700 cm^{-1} relative to ϵ_{000} appears to be unjustified.

B. IRUVDR experiments

In the infrared–ultraviolet double resonance experiments,[5–7] the CO_2 laser populates the (001) state, which rapidly equilibrates with the (100) state; then both levels decay according to the same double exponential function as is observed in infrared fluorescence experiments.[13,14] Equation (7) implies that the absorbance transient observed following laser excitation should be proportional to the excited stretching mode population and, thus, should obey the same time dependence. This behavior has previously been demonstrated in the 254 nm region,[5] and new measurements using interference filters at 289 and 313 nm also yield the same results. The rate constants for vibrational energy transfer measured

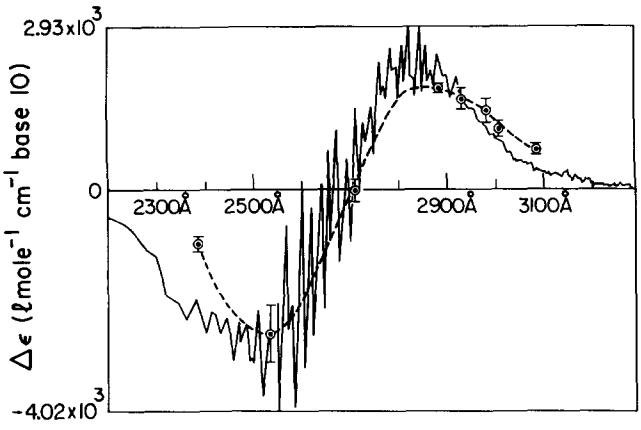

FIG. 3. Dependence of the magnitude of the IRUVDR transient upon wavelength. Solid curve is $\epsilon^* - \epsilon_{000}$, from the 200 and 333 K data of Ref. 11. The dashed curve connects the IRUVDR data points, the vertical scaling having been adjusted so that the amplitudes of the two curves are similar.

at all three wavelengths agree well with results obtained via infrared fluorescence,[13,14] as has been discussed previously.[5]

Another test of the assumption that $\epsilon_{010} \approx \epsilon_{000}$ can be derived from the wavelength dependence of the IRUVDR transients. According to Eq. (7) the change in the spectrum with temperature, being due solely to ozone excited in the stretching modes, should scale with the laser-induced transients. By adding a monochromator to the previously described apparatus,[5] we measured the magnitude of the initial transient at a number of wavelengths relative to that at 289 nm. We found that by using an appropriate scaling factor, the laser-induced transients could indeed approximate the temperature-induced absorbance change rather well, as is shown in Fig. 3. The slight red shift of the spectrum derived from IRUVDR relative to that derived from the temperature dependence may be due to a small quantity of multiply excited vibrational levels.

Several other IRUVDR measurements are capable of testing the spectral model developed here. One measurement involves choosing $\lambda = 271$ nm, where the instantaneous laser transient is found to be zero,[7] hence $\epsilon_{000} = \epsilon^*$. If ϵ_{010} were significantly different from ϵ_{000} at that wavelength, then a transient corresponding to (010) population would appear. However, none is observed, either in the current or in previous work.[7] A small, gradual, downward shift of the absorbance does occur on a relatively long time scale. We ascribe this to rarefaction of the sample caused by the temperature rise accompanying the $V \rightarrow T$ process.

Equation (7) may also be tested by an analysis of IRUVDR signals which possess a slow decay component, such as those at 3100 Å displayed in Refs. 6 and 7. This component has been assigned to thermally equilibrated ozone,[6] and its magnitude is therefore related to the quantity of vibrationally excited ozone initially formed. For the data of Refs. 6 and 7, Eq. (7) predicts a fractional excitation $[O_3^{\ddagger}]/[O_3]_{total}$ of 0.115 $\pm$ 0.020 based on the magnitude of the initial transient, and assuming a value for $\epsilon^*/\epsilon_{000} = 12 \pm 2$. In that range of excitation, the quantity of (100) plus (001) vibrationally excited ozone remaining after thermal equilibration is 0.10 of that initially produced by the laser pulse (in pure ozone), hence Eq. (7) predicts that the magnitude of the slow decay component should be 0.10 of that of the initial transient. Experimentally, the amplitude of the slow decay component is found to be 0.11 ± 0.03 of that of the initial transient, in excellent agreement with the preceding estimate. A potential complication would be the partial transparency induced by sample rarefaction, as discussed above, but at 310 nm this should affect the slow component by only about 10% of its magnitude, and can therefore be neglected. Thus, it is seen that Eq. (7) satisfactorily describes the absorbance at 310 nm over the range $0.01 \lesssim [O_3^{\ddagger}]/[O_3]_{total} \lesssim 0.1$.

A major difficulty in the determination of ϵ^* by the IRUVDR method is in measuring accurately the quantity of vibrationally excited ozone to which the UV absorbance transient corresponds. In principle, this can be done by observing attenuation of the infrared beam passing through the sample. This proved to be a difficult measurement under our normal experimental conditions, however. A beam attenuation measurement under conditions of high excitation is described below, in Sec. III B 1.

C. Comparison of absorption spectra of vibrationally excited ozone

According to Eq. (7), it is sufficient to determine $\epsilon^*(\nu)$ in order to explain satisfactorily the spectrum of ozone excited to low levels of excitation. There are two ways to obtain ϵ^*, the most direct being from the IRUVDR transients. The main difficulty is in the measurement of the quantity of vibrationally excited ozone formed in the laser pulse, as noted above. In the previous section we have estimated the fractional excitation for the experimental conditions of Refs. 6 and 7, viz. (0.115 ± 0.020), which fortuitously coincides with the value which was used therein in the determination of ϵ^*. The spectrum shows a broad peak at 2850 Å and falls off somewhat more sharply to the blue than to the red, reaching a near zero value at around 2500 Å.[7]

Another way to obtain ϵ^* is from the difference between spectra taken at different temperatures. Figure 4 depicts ϵ^* determined from the 333 and 200 K spectra of Simons *et al.*[11] Due to the weakness of the temperature dependence the spectrum is not highly accurate, especially away from the red end. A possible error in relative normalization of the original spectra would be especially troublesome, and a residue of structure in those spectra gives ϵ^* an artificially jagged appearance. Despite these deficiencies the spectrum is strikingly similar to the IRUVDR result of Ref. 7. The ϵ^* spectrum also bears a strong resemblance to the "ozone precursor" spectrum observed by several others during formation of ozone from oxygen at atmospheric pressure,[15,16] and which has been ascribed to vibrationally excited ozone.[16,17]

In summary, the approximate shape of the ϵ^* spec-

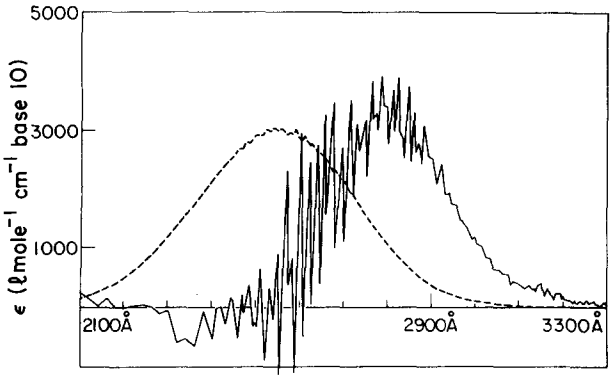

FIG. 4. The Hartley absorption spectrum of ozone. The dashed curve is the 200 K spectrum, and the solid curve is the vibrationally excited spectrum ϵ^*, a portion of which is displayed in Fig. 1.

trum has been determined from both the temperature dependence of the UV absorption spectrum and the IRUVDR measurements in Ref. 7. While more accurate data on the Hartley absorption continuum are clearly needed, the existing data are useful for a number of applications. Several such applications are discussed in the following section.

III. APPLICATIONS OF THE SPECTRAL MODEL

A. Rate constants for vibrational energy transfer

The alteration of the Hartley continuum caused by vibrational excitation finds a very useful application in the determination of rate constants for vibrational energy transfer by IRUVDR. Its extremely high sensitivity and the absence of systematic error may make it the method of choice for the study of relaxation rates for the singly excited vibrational levels of ozone, as has been discussed previously.[5] In Ref. 5, we estimated a crude lower limit for the rate of the rapid $\nu_3 \rightleftharpoons \nu_1$ equilibration process, on the order of 10^6 $\text{Torr}^{-1}\,\text{s}^{-1}$, from the "induction time" of the initial IRUVDR transient. These measurements have now been repeated at much lower ozone pressures, using an improved apparatus, employing collinear infrared and ultraviolet beams in either a 120 or a 20 cm cell, similar to the configuration of Ref. 6. Using an interference filter at 289 nm, the wavelength of greatest sensitivity, we were able to achieve a detection limit of about 10^{12} molecules cm^{-3} of $O_3^\ddagger$, by averaging over several hundred laser pulses. At a total pressure of 0.07 Torr the transient was observed to be essentially instantaneous to within the combined response time of the electronics and laser pulse width, around 1 or 2 μs. Thus, the previously reported induction time should be attributed to electronic interference from the laser, rather than to any kinetic process.

There are two possible explanations for the virtually instantaneous onset of the transient. One is that the $(001) \rightleftharpoons (100)$ equilibration occurs within the observed rise time, requiring a nearly gas kinetic collision rate. Since the energy transfer per collision is only 60 cm^{-1}, this explanation is certainly plausible. A second possible explanation is that $\epsilon_{100} \approx \epsilon_{001}$ at 289 nm, making the equilibration process incapable of observation. To distinguish between these hypotheses one should take measurements of comparable sensitivity over a range of wavelengths, it being unlikely that $\epsilon_{100} \approx \epsilon_{001}$ for all wavelengths. We have carried out some measurements in the 254 and 310 nm regions which yielded similar results as at 289 nm; however, due to lower sensitivity the ozone pressures required were several times greater. Thus, it is not possible to establish unambiguously a value for the $(001) \rightleftharpoons (100)$ equilibrium time from this experiment.

B. Vibrational energy deposition following CO_2 laser irradiation

The excitation of molecular species by high-intensity infrared radiation is a widely studied but still incompletely understood process.[18] At very high laser intensities, ozone is reported to undergo multiple-photon dissociation[19]; at lower intensities, such as those available from an unfocused CO_2 laser beam, the excitation process is surely less complex, but by the same token, the low-intensity excitation regime may be more readily understood, especially given the well-known spectroscopy of the low vibrational levels. The IRUVDR method provides a convenient and sensitive technique for measuring the fractional excitation of ozone $[O_3^\ddagger] / [O_3]_{\text{total}}$. We denote this quantity by $\langle n \rangle$, the mean number of IR photons absorbed by molecule, since at the low levels of excitation studied here the population of multiply excited ozone molecules is negligibly small. We present experimental results for $\langle n \rangle$ as a function of total pressure $(O_3 + O_2)$, and infrared frequency and fluence in the single-photon regime, along with model calculations which aid in interpreting the data.

1. *Experimental measurements*

Most of the data were obtained from measurement of the UV transient using a 289 nm interference filter. Collinear infrared and ultraviolet beams were employed in a $l = 20$ cm cell, care being taken to insure complete overlap of the UV beam by the IR beam. The sensitivity was sufficient to allow single-shot measurements of the transient. Infrared fluence passing through the rear iris with the cell evacuated was measured with a Scientech 380102 power meter. The fluence measurements represent an average over the beam area, the actual beam intensity displaying interference fringes resulting from passage through the irises and a germanium beam splitter. The ~20 nm bandwidth of the UV filter posed a potential problem due to wavelength variation of absorption coefficients of O_3 and $O_3^\ddagger$. Fortunately, however, the 289 nm wavelength lies near a flat portion of the $\Delta\epsilon = \epsilon^* - \epsilon_{000}$ curve (see Fig. 3). A reasonably well-determined value of $\Delta\epsilon \approx 2.6 \times 10^3$ $\ell\,\text{mol}^{-1}\,\text{cm}^{-1}$ (base 10) may be therefore assigned on the basis of the spectral model in order to relate the transient absorbance ΔA to the quantity of $O_3^\ddagger$ produced, via the equation $\Delta A = [O_3^\ddagger] l \Delta\epsilon$.

Despite the wealth of evidence presented earlier to support the basic validity of the spectral model, its

absolute accuracy has not yet been quantified. Hence, the value of $\Delta\epsilon$ cited above, and thus the corresponding value of $\langle n \rangle$, are of unknown accuracy. We therefore carried out a double check on the above method for determining $\langle n \rangle$ by using a sufficiently high pressure of O_3 and total pressure (~3 Torr O_3 in 10 Torr total pressure) to obtain measurable attenuation of the CO_2 laser beam during passage through the cell, thus establishing a direct determination of deposited infrared energy. Unfortunately, the UV optical density at that ozone pressure is too great to permit a simultaneous measurement of the 289 nm transient. We circumvented that problem by using a 313 nm interference filter instead, and scaling the ΔA value measured at 313 nm to a hypothetical value at 289 nm, using the previously measured ratio between the IRUVDR transients at these two wavelengths. The resulting value of $\langle n \rangle$ was about 40% lower than that determined directly by infrared transmission in two separate experiments. Considering the uncertainties in the measurements and in the value of $\Delta\epsilon$, and in view of the possible influence of multiply excited vibrational levels ($\langle n \rangle$ was about 0.2 in these measurements), this agreement is tolerable.

We conclude that the technique of determining $\langle n \rangle$ from IRUVDR transients may be subject to a systematic error of up to 40%. However, as it is likely that much of this discrepancy is related to the conditions employed in this particular experiment, the data which follow, taken at lower degrees of excitation and using the 289 nm bandpass filter, are probably of considerably better accuracy. The precision of an individual measurement, arising principally from variations in infrared laser fluence passing through the cell, is on the order of ± 20%.

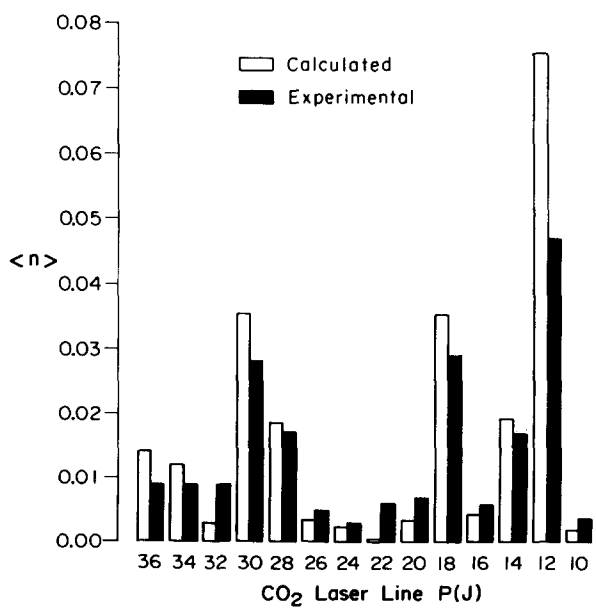

FIG. 5. Mean fractional excitation of ozone by CO_2 laser irradiation for different laser lines in the 9.6 μm P branch. Solid bars denote experimental data, open bars denote model calculations (see the text). Ozone pressure is 0.6 Torr, oxygen pressure is 2.4 Torr. The experimental laser fluence is 0.04–0.06 J/cm^2 for these lines, 0.05 J/cm^2 being used in the model calculations.

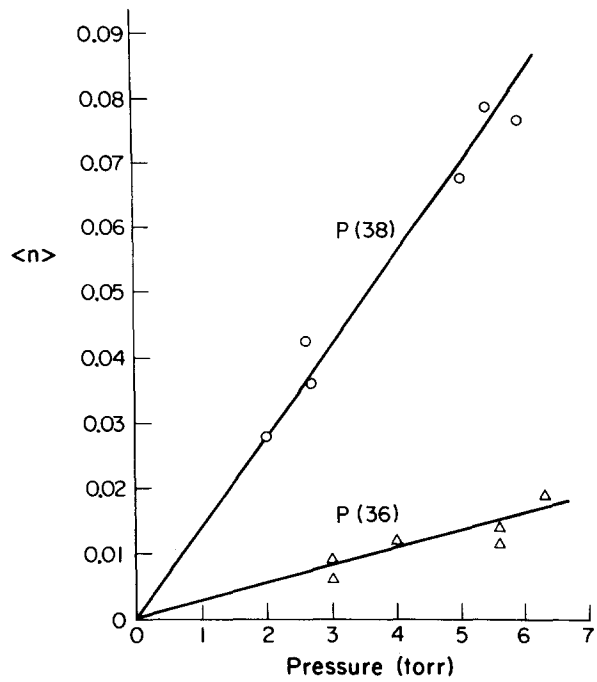

FIG. 6. Experimental dependence of $\langle n \rangle$ upon total pressure, for CO_2 $P(36)$ and $P(38)$ lines, at a fluence of 0.034 J/cm^2, and a composition of 10% ozone in oxygen.

Typical experimental results for $\langle n \rangle$ are depicted in Figs. 5 through 7. Pumping of ozone was observed using *all* of the available CO_2 laser lines in the 9.6 μm P branch, the strongest pumping occurring with lines, such as $P(12)$ and $P(30)$, that are resonant with O_3 absorption lines (see Fig. 5). With a sampling of both on- and off-resonant laser lines, we found $\langle n \rangle$ to be linearly proportional to total pressure (at a fixed ozone mole fraction) to within experimental error in the 2 to 6 Torr range studied (see Fig. 6). The dependence of $\langle n \rangle$ upon laser fluence was studied by attenuating the laser beam with polyethylene sheets. With several off-resonant lines, the signal was found to be linearly proportional to fluence, but with on-resonant lines the amplitude of the IRUVDR transient showed marked saturation behavior, as is shown in Fig. 7.

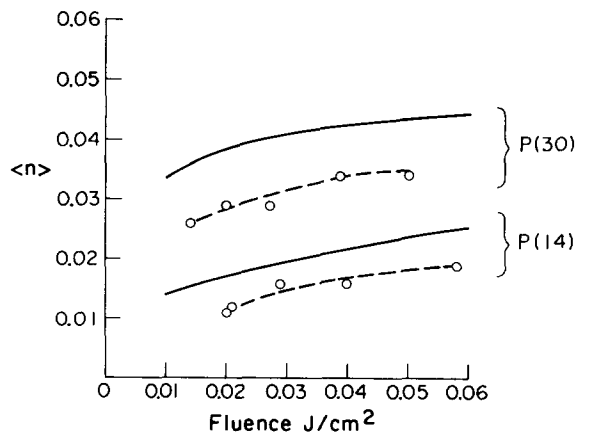

FIG. 7. Dependence of $\langle n \rangle$ upon laser fluence for on-resonance CO_2 laser lines. Solid curves denote model calculations (see the text).

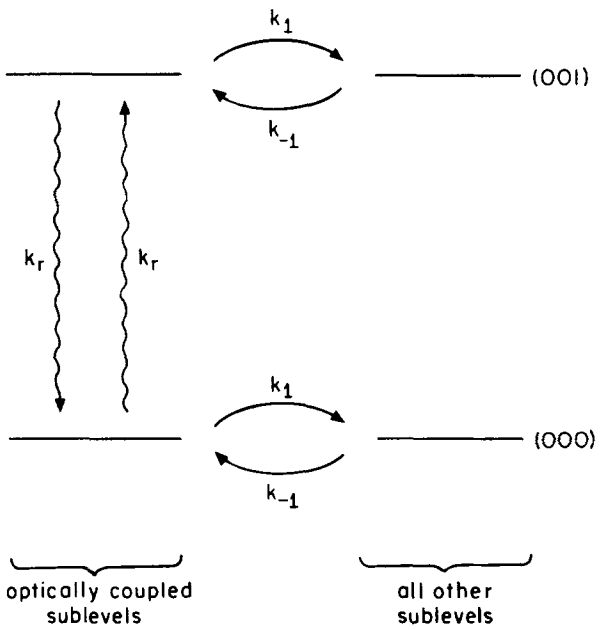

FIG. 8. Kinetic model for vibrational excitation of ozone in the laser field.

The dependence of $\langle n \rangle$ upon mole fraction of ozone was not explored, dilute mixtures of ozone in oxygen being used in most measurements. However, some observations were made using the CO_2 $P(30)$ line and the apparatus described in Ref. 5, which demonstrated decreasing values of $\langle n \rangle$ with increasing ozone concentration, especially at high values of $\langle n \rangle$. This may be due to attenuation of the laser beam upon transmission through the sample. As the ozone absorption lines are quite narrow, they may be capable of selectively absorbing the most closely resonant frequency components of the CO_2 laser output, thus "burning a hole" in the laser's output spectrum. This point is discussed more fully in the following section.

2. *Excitation model*

In order to gain insight into the experimental results, we have carried out some model calculations for $\langle n \rangle$. The kinetic scheme utilized is depicted in Fig. 8. In brief, the upper and lower rotational sublevels associated with an ozone absorption line near the laser frequency are optically coupled to each other in the presence of the laser field by the radiative rate constant k_r, and are assumed to be collisionally coupled to the remaining rotational sublevels in each vibrational state by the pseudo-first-order rate constants k_1 and k_{-1}. This "four-box" model has been previously employed by us to describe the kinetics of infrared saturation,[20] passive Q switching,[21] and infrared double-resonance experiments employing CO_2 lasers[22] and tunable diode lasers.[23] In the pressure range of interest here, vibrational deactivation during the ~1 μs laser pulse may be neglected.

While the model depicted in Fig. 8 may be solved exactly,[22] a much less cumbersome and sufficiently accurate solution is the following expression, derived by assuming steady-state concentration in the optically coupled sublevels

$$\frac{d\langle n \rangle}{dt} = \frac{\beta k_1/2}{1 + k_1/2k_r} , \tag{9}$$

where $\beta = k_{-1}/(k_1 + k_{-1})$, the equilibrium population in the pumped rotational sublevel. Integrating over the laser pulse duration and summing over all ozone absorption lines which appreciably interact with the laser radiation yields the net $\langle n \rangle$ value. (In practice, only lines within about 0.1 cm^{-1} of the laser frequency need to be included for the maximum fluence considered here, approximately 0.05 J/cm^2.) The radiative rate constant k_r can be written as[24]

$$k_r = I\sigma(\tilde{\nu})/h\nu\beta \tag{10}$$

for monochromatic radiation. In the present situation, Eq. (10) must be modified to take account of the distribution of frequencies in the laser output arising from the longitudinal mode structure. This can be done by integrating Eq. (10) over a normalized intensity distribution function $I(\tilde{\nu})$, to be specified a little later, giving

$$k_r = \int I(\tilde{\nu})\,\sigma(\tilde{\nu})\,d\tilde{\nu}/h\nu\beta , \tag{11}$$

where $\tilde{\nu}$ denotes wave number in cm^{-1}, $I(\tilde{\nu})$ is the radiation intensity in W per cm^2 per cm^{-1}, and $\sigma(\tilde{\nu})$ is the photon absorption cross section in cm^2 per cm^{-1}. The cross section $\sigma(\tilde{\nu})$ may be approximated by the homogeneous line shape function

$$\sigma(\tilde{\nu}) = \frac{S}{\pi}\left[\frac{\delta\tilde{\nu}}{(\tilde{\nu} - \tilde{\nu}_0)^2 + (\delta\tilde{\nu})^2}\right] , \tag{12}$$

where S is the integrated line strength in cm^2, $\tilde{\nu}_0$ the resonant wave number, and $\delta\tilde{\nu}$ is the half-width at half-height of the absorption line. We assume that inhomogeneous broadening may be neglected.

The usual Lorentzian power-broadened line shape expression for absorbed energy versus detuning[24,25] may be obtained by combining Eqs. (9), (10), and (12). The use of Eq. (11) instead of Eq. (10) simply gives a broader function. No attempt is made to include the effect of laser beam attenuation; thus, this treatment is applicable only to optically thin samples.

It remains to find appropriate input parameters for the above equations. The linewidth $\delta\tilde{\nu}$ is taken as the collision-broadened half-width, found to be 0.06 $cm^{-1}\,atm^{-1}$ for O_3–O_2 collisions and 0.15 $cm^{-1}\,atm^{-1}$ for O_3–O_3 collisions.[26] The ozone line positions are taken from Ref. 27, and the integrated line intensities are from the same reference, but multiplied by 1.113, in accordance with more recent work.[28] The population relaxation rate constant k_1 was set equal to the dephasing rate constant $k_2 = 2\pi c\delta\tilde{\nu}$ in accordance with observations on similar molecules.[29] The temporal shape of the laser pulse is an important input variable; we determined this experimentally with a photon-drag detector. It is a typical "TEA-laser" pulse profile, with an initial spike of 40–50 ns duration containing ~60% of the total pulse energy, and a low-intensity tail, lasting a little less than 1 μs, containing 40% of the pulse energy. For

modeling purposes, this was approximated as a flat-topped spike followed by a flat tail lasting ten times the spike duration, with the intensities adjusted to give the proper fluence ratios. Best results were obtained with a total pulse duration of 0.5 μs, which is somewhat shorter than the observed pulse length. The use of the shorter tail duration may be rationalized in either of two ways. First, it may be correct for the presence of oscillatory mode structure present in the actual pulse shape, which may compress the effective time during which the laser is on. An alternative rationale is that decreasing the effective pulse duration may instead be a means of compensating for a discrepancy between k_1 and k_2; halving the pulse duration is, in fact, equivalent to using a k_1/k_2 ratio of 0.5.

The remaining parameter which required trial-and-error fitting concerned the laser intensity distribution function $I(\bar{\nu})$; the choice of this parameter particularly influenced the degree of off-resonance pumping. The laser line shape is expected *a priori* to consist of narrow cavity modes with a spacing of 0.005 cm^{-1}, within an intensity envelope that follows the pressure-broadened line shape (0.05 cm^{-1} FWHM for the laser gas mixture used), which is truncated at the zero-gain threshold.[32] Since the precise locations of the modes are unknown, and most likely vary during the course of the experiment, we felt it best to ignore structure entirely and use a smooth line shape function $I(\bar{\nu})$. Results obtained using a truncated Lorentzian line shape were found to differ little from those obtained using a triangular line shape having the same width at the base. The triangular line shape has the advantage of yielding an analytical solution to Eq. (11). We found that the values of $\langle n \rangle$ found for off-resonance laser lines was very sensitive to the assumed base width, but that with the on-resonance lines this parameter was not critical. The calculations presented in Figs. 5 through 7 assume a base full width of 0.028 cm^{-1}.

The agreement between experimental and calculated values of $\langle n \rangle$ is, on the whole, rather satisfactory, although the quality of the fit varies from line to line (see Fig. 5). The dependence of $\langle n \rangle$ upon k_1 (hence, pressure at fixed O_3 mole fraction) is predicted to be essentially linear for most CO_2 laser lines, in agreement with the experimental findings (see Fig. 6). This is explained in the case of on-resonance pumping by collisional alleviation of rotational hole burning. For off-resonant laser lines, pressure broadening of the absorption line shape becomes the most important effect. The dependence of $\langle n \rangle$ upon fluence is predicted to be linear for off-resonance pumping, in agreement with the experiment. On the other hand, the fluence dependence is markedly nonlinear for on- and near-resonant laser lines which saturate individual absorptions in the sample; the model predicts these lines to be the CO_2 9 μm $P(12)$, $P(14)$, $P(18)$, $P(30)$, and $P(38)$ lines. Saturation has indeed been confirmed experimentally for all of these lines, selected data appearing in Fig. 7.

In summary, the degree of vibrational excitation of O_3 by unfocused pulsed CO_2-laser radiation may be predicted for a wide range of conditions by using model calculations to extend the range of experimental data. With refined input parameters, especially regarding the characterization of the laser radiation, and by inclusion of beam attenuation through the sample, even better agreement between experiment and calculation may be anticipated.

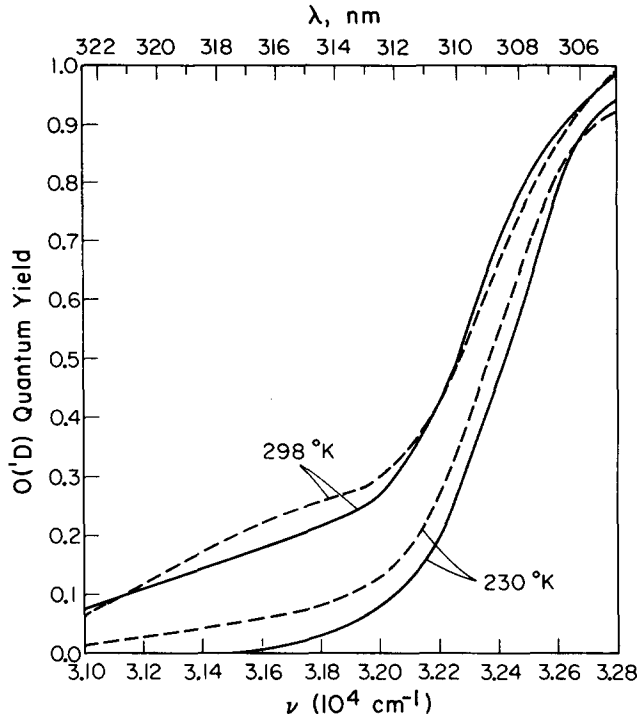

FIG. 9. $O(^1D)$ quantum yields vs photolysis wavelength. Solid lines are experimental determinations (Refs. 34 and 35) and dashed lines are from the model calculations described in the text. Note that the Brock and Watson data (Ref. 34) have been renormalized to unity at 304 nm.

C. $O(^1D)$ formation in the near ultraviolet photolysis of ozone

The photolysis of ozone in the Huggins–Hartley ultraviolet region yields both $O(^1D)$ and $O(^3P)$ atoms; in the stratosphere, the $O(^1D)$ atoms thus formed are the major source of OH radicals. Much interest has, therefore, focused on the quantum yield for $O(^1D)$ production from ozone photolysis, especially in the "fall off region" of 300–320 nm where considerable ultraviolet flux penetrates the lower altitudes.[33–36] In this fall off region it is found that the $O(^1D)$ quantum yield declines rapidly from a value close to unity at 300 nm towards a negligibly small value near 320 nm, the precise position and steepness of the decline being strongly temperature dependent[33,34] (see Fig. 9). The ability to model these data is important, not only in terms of parametrizing the quantum yield function for a wide range of wavelengths and temperatures, but also in providing an understanding of the photolysis mechanism.

Previous attempts at modeling the fall off region data have focused primarily on the role of rotational energy in contributing to the total energy required to reach the $O(^1D)$ production threshold. However, ro-

tational energy alone does not explain the observed temperature dependence.[33] Recent investigations have suggested that vibrational excitation is also important in the photolysis process. Zittel and Little[37] have observed a greatly enhanced $O(^1D)$ production cross section in the red end of the Hartley band following IR laser excitation. They ascribe this effect to vibrationally excited ozone having a large absorption cross section in that spectral region. The temperature dependence of the absorption coefficient, as seen, e.g., in the data of Ref. 11, is consistent with that premise. Hudson[38] has utilized those absorption data in quantum yield model calculations which give good agreement with experiment. A drawback of those calculations is that, unfortunately, the absorption data alone are not sufficient to specify uniquely a spectroscopic model for the ozone ultraviolet spectrum.

In this paper, we have presented a model for the Hartley absorption spectrum of vibrationally excited ozone, based on Eq. (7), which is well-supported by the IRUVDR experiments, and thus can provide a reasonable starting point for $O(^1D)$ quantum yield modeling. Extension of Eq. (7) into the longer wavelength Huggins region poses no conceptual problem, even if, as has been proposed,[39] the Huggins bands belong to another electronic transition. This is because we can reasonably assume that, in the fall off region, the major contribution to the vibrationally excited spectrum is the tail of the (100) plus (001) excited ozone spectrum depicted in Fig. 4, and belonging to the Hartley transition. Even further to the red, where the "hot" Huggins spectrum appears to be discrete, it is still found that transitions originating from (100)- and (001)-excited ozone possess greater intensity than those originating from (010),[40] and thus dominate the spectrum of vibrationally excited ozone.

Proceeding with the calculation according to the method of Moortgat *et al.*[33] we assume that the total internal energy (vibrational plus rotational) adds fully to the energy acquired from the ultraviolet photon, and that for a given total energy the $O(^1D)$ quantum yield varies as a ramp function from zero at a selected threshold energy to unity at a higher energy, taken here to be 600 cm^{-1} above the threshold. The classical density of rotational states $\propto (E_{rot})^{1/2}$ is fully satisfactory for this

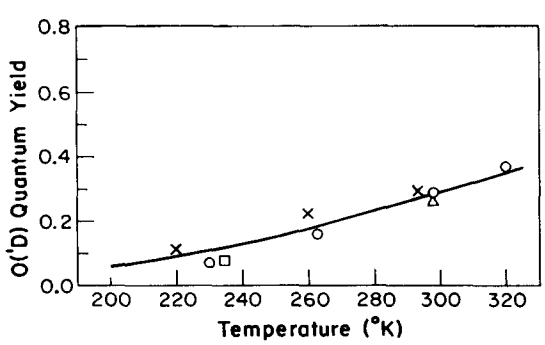

FIG. 10. $O(^1D)$ quantum yields at 313 nm vs temperature. o = Ref. 33 data, Δ = Ref. 34, □ = Ref. 35, × = Ref. 36; solid line is the model calculation described in the text.

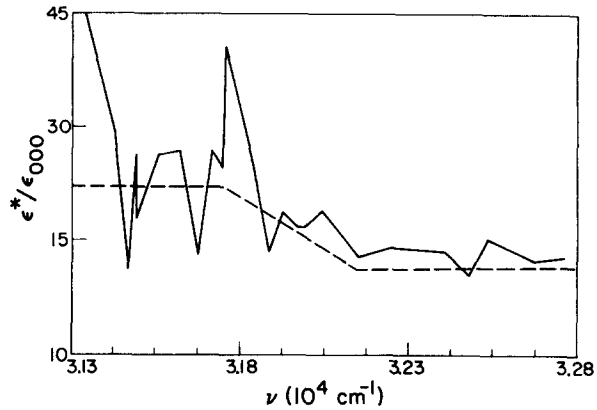

FIG. 11. The ratio $\epsilon^*/\epsilon_{000}$ in the 31 300–32 800 cm^{-1} region (solid curve). For purposes of modeling the $O(^1D)$ photodissociation quantum yield, as described in the text, the smooth dashed curve is used instead.

calculation. The quantum yield for the ground, first excited stretching and first excited bending levels are computed separately, weighted according to their absorption coefficient and population, and combined to give the net $O(^1D)$ quantum yield $\bar{Q}$ as follows:

$$\bar{Q} = \frac{\Sigma \epsilon_{ijk} P_{ijk} Q_{ijk}}{\Sigma \epsilon_{ijk} P_{ijk}} , \tag{13}$$

where ϵ_{ijk}, P_{ijk}, and Q_{ijk} are the absorption coefficient, population and $O(^1D)$ quantum yield, respectively, of the (ijk) vibrational level. According to Eq. (7), this reduces to

$$\bar{Q} = \frac{\epsilon_{000}(P_{000} Q_{000} + P_{010} Q_{010}) + \epsilon^* P^* Q^*}{\epsilon_{000}(1 - P^*) + \epsilon^* P^*} , \tag{14}$$

where $P^* = P_{100} + P_{001}$. The above equation requires knowledge of ϵ^*/ϵ_0 in the fall off region, which is taken to be the ramp function depicted in Fig. 11. The $O(^1D)$ threshold energy was adjusted for best fit between calculations and experiments, yielding a value of (32 900 ± 100) cm^{-1}.

The comparison of experimental and calculated results appears in Figs. 9 and 10. Good agreement is seen in the wavelength dependence of the quantum yield over the 305–322 nm range at both low and room temperatures. At 313 nm, the agreement between the calculation and a large number of experimental results is excellent over the full temperature range studied. It should be noted, however, that the long wavelength tail above 313 nm, appearing in the Brock and Watson[34] data depicted in Fig. 9 and predicted as well by this calculation, conflicts with the majority of experimental studies, which instead show a more rapid decline of the quantum yield. Until this issue is resolved the validity of the model calculation remains open to question. Its success at and below 313 nm does, however, suggest that vibrationally excited ozone does indeed play an important role in stratospheric ozone photolysis.

IV. CONCLUSIONS

A model for the Hartley ultraviolet spectrum of vibrationally excited ozone has been presented and applied to

problems involving vibrational energy transfer, infrared energy deposition resulting from pumping by a CO_2 laser, and stratospheric ozone photodissociation. In the latter instances, simple models have been presented which are capable of reproducing the experimental results quite well. Many other molecules possess strong, continuous ultraviolet absorption spectra, as well as infrared resonances near CO_2 laser lines; the alkyl halides are just one example.[41] Many of these species may therefore be excellent candidates for study by the methods described here.

ACKNOWLEDGMENTS

This work was supported by the Air Force Geophysics Laboratory under Contract No. F19628-80-C-0028. We would like to thank Dr. R. Pack, Dr. R. Hudson, and Dr. E. Bair for helpful discussions.

[1]H. Okabe, *Photochemistry of Small Molecules* (Wiley, New York, 1978).
[2]C. W. von Rosenberg, Jr., and D. W. Trainor, J. Chem. Phys. **61**, 2442 (1975).
[3]C. W. von Rosenberg, Jr., and D. W. Trainor, J. Chem. Phys. **63**, 5348 (1975).
[4]W. T. Rawlins, G. E. Caledonia, and J. P. Kennealy, J. Geophys. Res. **86**, 5247 (1981).
[5]S. M. Adler-Golden and J. I. Steinfeld, Chem. Phys. Lett. **76**, 479 (1980).
[6]I. C. McDade and W. D. McGrath, Chem. Phys. Lett. **72**, 432 (1980).
[7]I. C. McDade and W. D. McGrath, Chem. Phys. Lett. **73**, 413 (1980).
[8]P. J. Hay and T. H. Dunning, J. Chem. Phys. **67**, 2290 (1977).
[9]S. M. Adler-Golden, Chem. Phys. (in press).
[10]R. K. Sparks, L. R. Carlson, K. Shobatake, M. L. Kowalczyk, and Y. T. Lee, J. Chem. Phys. **72**, 1401 (1980).
[11]J. W. Simons, R. J. Paur, H. A. Webster III, and E. J. Bair, J. Chem. Phys. **59**, 1203 (1973).
[12]T. Kleindienst and E. J. Bair, Chem. Phys. Lett. **49**, 338 (1977).
[13]D. I. Rosen and T. A. Cool, J. Chem. Phys. **62**, 466 (1975).
[14]G. A. West, R. E. Weston, Jr., and G. W. Flynn, Chem. Phys. Lett. **56**, 429 (1978).
[15]J. F. Riley and R. W. Cahill, J. Chem. Phys. **52**, 3297 (1970).
[16]C. J. Hochanadel, J. A. Ghormley, and J. W. Boyle, J. Chem. Phys. **48**, 2416 (1968).
[17]T. Kleindienst, J. R. Locker, and E. J. Bair, J. Photochem. **12**, 67 (1980).
[18]H. W. Galbraith and J. R. Ackerhalt, in *Laser-Induced Chemical Processes*, edited by J. I. Steinfeld (Plenum, New York, 1981), pp. 1–44; C. D. Cantrell, S. M. Freund, and J. L. Lyman, in *The Laser Handbook*, edited by M. L. Stitch (North–Holland, Amsterdam, 1979), Vol. 3, pp. 485–576.
[19]D. Proch and H. Schröder, Chem. Phys. Lett. **61**, 426 (1979).
[20]I. Burak, J. I. Steinfeld, and D. G. Sutton, J. Quant. Spectrosc. Radiat. Transfer **9**, 959 (1969).
[21]I. Burak, P. L. Houston, D. G. Sutton, and J. I. Steinfeld, IEEE J. Quantum Electron. **7**, 73 (1971).
[22]J. I. Steinfeld, I. Burak, D. G. Sutton, and A. V. Nowak, J. Chem. Phys. **52**, 5421 (1970).
[23]C. C. Jensen, T. G. Anderson, C. Reiser, and J. I. Steinfeld, J. Chem. Phys. **71**, 3648 (1979).
[24]J. Steinfeld, *Molecules and Radiation* (MIT, Cambridge, 1977), p. 27.
[25]J. I. Steinfeld and P. L. Houston, "Double-Resonance Spectroscopy," in *Laser and Coherence Spectroscopy*, edited by J. I. Steinfeld (Plenum, New York, 1978), p. 16.
[26]A. Barbe, 36th Symposium on Molecular Spectroscopy, Ohio State University, Columbus, Ohio, June 15–19, 1981.
[27]A. Barbe, C. Secroun, P. Jouve, N. Monnanteuil, J. C. Depannemaecker, B. Duterage, J. Bellet, and P. Pinson, J. Mol. Spectrosc. **64**, 343 (1977).
[28]C. Secroun, A. Barbe, and P. Jouve, J. Mol. Spectrosc. **85**, 8 (1981).
[29]Only a small number of $T_1:T_2$ measurements have been performed on infrared transitions (Ref. 25). Delayed nutation experiments have indicated that the cross sections for population and phase relaxation are the same for NH_3 (Ref. 30) and CH_3F (Ref. 31). Analysis of the diode–infrared laser-double resonance experiments in SF_6 (Ref. 23) indicates that the cross sections for the two processes do not differ by more than 40%.
[30]G. M. Dobbs, R. H. Micheels, J. I. Steinfeld, J. H-S. Wang, and J. M. Levy, J. Chem. Phys. **63**, 1904 (1975).
[31]P. R. Berman, J. M. Levy, and R. G. Brewer, Phys. Rev. A **11**, 1668 (1975).
[32]C. Young and R. H. L. Bunner, Appl. Opt. **13**, 1438 (1974).
[33]G. K. Moortgat, E. Kudszus, and P. Warneck, J. Chem. Soc. Faraday Trans. 2 **73**, 1216 (1977).
[34]J. C. Brock and R. T. Watson, Chem. Phys. **46**, 477 (1980).
[35]C. L. Lin and W. B. DeMore, J. Photochem. **2**, 161 (1973).
[36]S. Kuis, R. Simonaitis, and J. Heicklen, J. Geophys. Res. **80**, 1328 (1975).
[37]P. F. Zittel and D. D. Little, J. Chem. Phys. **72**, 5900 (1980).
[38]R. Hudson, *Proceedings of the Quadrennial International Ozone Symposium*, edited by J. London (IAMAP, Boulder, 1980), Vol. I, pp. 146–152.
[39]J. C. D. Brand, K. J. Cross, and A. R. Hoy, Can. J. Phys. **56**, 327 (1978).
[40]D. H. Katayama, J. Chem. Phys. **71**, 815 (1979).
[41]T. D. Padrick, A. K. Hays, and M. A. Palmer, Chem. Phys. Lett. **70**, 63 (1980).